

HINGELESS ROTOR DYNAMICS IN HIGH SPEED FLIGHT

H. Huber and H. Strehlow

Messerschmitt-Bölkow-Blohm GmbH  
Ottobrunn - Germany

Summary

A high speed flight research program has been carried out to determine the MBB BO 105 Hingeless Rotor behaviour within an expanded flight envelope. True Airspeeds of 200 knots (pure helicopter version) and of 218 knots (winged helicopter version) were achieved in dive conditions, corresponding to advance ratios up to 0.53 and advancing blade tip Mach numbers up to 0.97. Rotor blade versions with constant thickness airfoil, and with thin tip modifications were evaluated.

The paper discusses the essential test results in comparison to theoretical investigations. Main emphasis is placed upon findings in the areas of rotor structural loads, control and stability behaviour, and aeroelastic stability characteristics. In connection with the existing scope of experience the outcomes of the program provide a continuous picture of hingeless rotor characteristics over a wide speed and maneuver range.

1. Introduction

Substantial research, development, and operational experience during recent years have made the hingeless rotorcraft an accepted production aircraft. The helicopter BO 105 - flown for the first time in 1967 and in series production since 1971 - incorporates the well known MBB hingeless rotor system, classified as a soft flapwise, soft inplane type of rotor. While originally designed for the BO 105, the concept is of course interesting for future high performance rotorcraft projects which will exceed the existing scope of experience. It therefore was desirable to obtain an insight into an extended speed and maneuver envelope and to establish real limitations of the system.

In 1972 a High Speed Flight Research Program, sponsored in part by the Ministry of Defence of the Federal Republic of Germany, was started. The two main objectives of this program were

- to determine the MBB hingeless rotor system behaviour within an extended flight envelope (high thrust, high advance ratio, high advancing-blade tip Mach number)
- and to investigate advanced blade modifications on this rotor type.

For this program a BO 105 helicopter was modified into a high-performance configuration, designated the "Hochgeschwindigkeitshubschrauber BO 105 HGH". Figure 1 gives a picture of the pure helicopter configuration in flight. The modifications were mainly aimed to a reduction of drag, to an improvement of basic stability characteristics, and to an increase of fatigue strength of some components of the control system. Later in the program the test vehicle was modified to include a wing with in-flight controllable speed brakes.

This paper doesn't deal with the whole program performed, but will concentrate on some essential results of hingeless rotor dynamics, such as rotor loads, flight behaviour, and aeroelastic stability characteristics. The outcomes will be considered as a continuation to previous theoretical and experimental experience in order to get a more complete picture of rotor behaviour within a wide flight envelope. An outline of the more practical aspects of the high speed flight pro-

gram is given in Reference 1.

## 2. Short Description of Test Vehicle and Test Program

In the following section a short description of the HGH test vehicle as well as of the flight test program is given, as far as it is necessary for the discussion of the succeeding results. More details are given in Reference 1.

### 2.1 Test Vehicle

Fuselage: The HGH fuselage, shown in Figure 1 is basically a standard BO 105 fuselage with modifications mainly aimed to a reduction of drag and to an improvement of basic stability characteristics. These included a rear fuselage fairing, a rotor head fairing, a shortened undercarriage, and different tailplane configurations. To investigate the effects of load sharing the aircraft was later modified to include a wing with an area of 64 square feet which could provide a 30 percent deloading of the rotor. The winged version of the HGH is shown in Figure 2.

Rotor and Control System: Main and tail rotor were identical to the standard BO 105 system. The main rotor can be classified as a stiff hub hingeless rotor with soft flapwise, soft inplane type of blades (Reference 2). Fundamental frequency ratios of 1.12 in flapwise and 0.65 in inplane direction are two descriptive parameters of this fourbladed rotor system. Two different types of rotor blades were evaluated during the flight test program:

- the standard rotor blade with constant NACA 23012 mod. airfoil section
- and a thin-tip blade (AGB-I) with NACA 23012 mod. airfoil section up to 70% radial station and a linear taper in thickness to a V 13006-0.7 airfoil at the tip.

The control system was identical to the standard aircraft, with the exception of slightly strengthened control rods and swashplate. This was done for safety precaution. A stability augmentation system was not installed in the aircraft.

### 2.2 Test Program

The flight test program was basically divided into three sections:

- A first section served to optimize certain fuselage and tail-plane modifications and to establish rough flight envelopes. With a gross weight of 4200 lb a maximum flight speed of 180 knots was reached in a dive flight condition.
- The main flight program of the pure helicopter version was performed with a gross weight of 5070 lb. A maximum flight speed of 173 knots was obtained with standard blades and a speed of 200 knots with thin tip blades.
- The third section was performed with the winged helicopter version, achieving a maximum dive speed of 218 knots.

Since the engine power installed in the BO 105 is not sufficient for the desired speed range in level flight, the technique used in flight testing was to use constant power setting and to achieve speed points up to maximum speed in dive flight conditions. The aircraft was trimmed at about 80 percent of maximum shaft horsepower, equivalent to approximately 145 knots horizontal flight collec-

tive trim setting. Test data were mainly obtained at a density altitude of 5000 feet.

### 3. Rotor Envelope

The extension of rotorcraft usage is widely restricted by their narrow flight envelope. Penetration into deep stall and/or occurrence of compressible phenomena are the classical limitations of thrust and speed. Additional impacts can result from flight behaviour, from vibratory or aeroelastic phenomena, and other problems. One main objective of the high speed research program was to establish the flight envelope boundaries of the hingeless rotor system under consideration of all potential limitations mentioned above.

Presented in Figure 3 is the flight envelope which was achieved during the test program. In the  $C_T/\sigma$  versus  $\mu$  diagram boundaries for the rotor with two different blade versions are shown. In general, maximum maneuver points in the low to medium range were obtained in steady state turns, maneuver points in the upper range were flown as transient conditions during symmetrical pull-out maneuvers for recovery from the maximum flight speed conditions. Boundaries in the lower speed range were primarily due to rotor stall limits and the corresponding increase of control loads, whereas limitations in the maximum speed range were caused to some extent by the provision for a safe recovery out of the extreme dive conditions. An aeroelastic phenomenon encountered at this boundary will be discussed later in more detail.

Within this rotor flight envelope the following peak values of advance ratio and advancing-blade tip Mach number were achieved:

	STANDARD BLADES	THIN TIP BLADES	
$\mu$	0.43	0.46	0.53 <sup>+) </sup>
$M_{1,90^\circ}$	0.93	0.96	0.97 <sup>+) </sup>

<sup>+)</sup>  winged helicopter version

### 4. Rotor Structural Loads

Hingeless rotor systems are, in general, capable to produce and to transfer large moments from the blades to the hub and into the fuselage. This high moment capacity gives a different situation for the loading conditions compared to articulated rotors (see Reference 3). For example, the trim behaviour with the hingeless rotor is characterized by the fact that an inclination of the thrust vector is always combined with a strong moment action directly at the hub which provides the main contribution to the trim requirements around the center of gravity.

This capability of producing large moments results of course in higher rotor and blade loads; the most stressed sections being the hub and the blade attachment. One main objective of the program was to determine the loading conditions of the hingeless rotor system within the extended speed and maneuver range, and furthermore to recognize possible structural limitations resulting for example from rotor moments, control loads or vibratory loads.

#### 4.1 Bending Moments

Measured and calculated rotor and blade moment data are shown in Figures 4 to 6. Data for normal 1g-flight condition and for maneuvers are collected in these diagrams in order to give a concentrated overview about the loading behaviour. The development of the hub moment over speed, shown in Figure 4, represents the trim requirements for the constant power flight conditions, where an increase of rotor moments with increasing speed is necessary to overcome the significant tailplane contribution due to the high rate of descent. For a medium aircraft c.g. location the hub bending moments remain below 80% of endurance limit at maximum dive speed. This level rises rapidly with load factor. However, fatigue limits were reached only during some excessive pull-out maneuvers for recovery from maximum speed points. A nearly identical loading behaviour is found for the flap bending moments at the blade root section, see Fig. 5.

The chordwise bending moments at a 14% radial station are indicated by Figure 6. The oscillatory moments, which are determined basically by blade dynamics, show agreement with flap bending load behaviour for steady flight conditions. At the maximum dive flight speed of 200 knots stresses in the blade root sections reached only 60% of endurance limit. Lift sharing between rotor and wing proved to reduce the chordwise oscillatory loads significantly (Figure 6), an effect, which is attributable to a reduced Coriolis-excitation with lower blade coning.

Considering the large number of parameters involved in a complete treatment of aircraft trim and loading calculation procedure and considering also the extreme flight conditions investigated, the agreement between calculated and measured bending loads is good. In summary one can conclude that the aeroelastic rotor theory with the simplified straight blade model for hingeless rotors (Reference 4) is able to provide reasonably accurate the lower harmonic dynamic loads, even for extreme flight conditions.

#### 4.2 Control Loads

Loading of the pitch link, which reacts on the blade aerodynamic and dynamic pitching moments, usually is one of the main restrictions on helicopter flight envelope expansion. Alternating pitch link loads typically show a rapid increase when blade stall or severe compressibility are reached. With a proper component sizing it seems to be not a strength and fatigue problem of the pitch links themselves, but a sharp load rise may be a sign that the rotor is near its aerodynamic limitations.

From the pure aerodynamic standpoint, hingeless rotor systems do not significantly differ from conventional systems. However, main flexibilities and partially strong elastical couplings may result in additional effects. For example, different locations of the main flexibilities with respect to the pitch bearing can more or less influence the control loads of the rotor. The BO 105 hingeless rotor with the pitch bearing close to the hub arms and with all blade bending outboard is an elastically coupled system (References 4, 5). One important aspect was, to get more information about the control loads behaviour of this type of rotor system within the extended flight envelope.

Oscillatory control loads for the thin tip blades (AGB I) were evaluated and are shown by Figure 7 for the flight conditions considered before. As can be seen, there is no dramatic increase in control loads up to maximum dive speed. A waveform analysis shows that within the normal 1g-flight envelope control loads are mainly influenced by the moment characteristics of the airfoil. With increasing airspeed the impulsive loading associated with transonic flow conditions on the advancing side of the rotor causes strong nose-down moments and correspondingly high control loads within the range of the advancing blade. A simulated

aerodynamic environment with strong shock fronts will be shown in Figure 9.

Typical stalling conditions are reached during maneuvers, where control loads exhibit the usual sharp increase with significant harmonics of multiples of rotor frequency. Pull-out maneuvers from maximum speeds were partially limited by these pitch link loads. As expected, the standard blades were superior to the thin tip blades in this regard, leading to a higher thrust capability of 0.25 g at speeds around 130 - 140 knots (compare Figure 3). It was found, however, that the disadvantage of thin tip blades decreases with higher airspeeds and it can be concluded that beyond a certain value of advancing-blade tip Mach number a safe rotor operation is only possible with thinned-tip blades.

## 5. Handling Characteristics

As mentioned before, due to limited BO 105 engines power available, high speed points could only be achieved in strong dive conditions. Figure 8 shows some important flight parameters over speed range. With collective pitch almost constant the vertical speed components in maximum dive are rather high. For example, the flight path angle at the maximum speed point of 218 knots with the winged version is in the magnitude of -20 degrees, with a pitch attitude of about -25 degrees. It becomes obvious from these values, that a exploration of such an expanded flight envelope was only possible under the precondition of a highly controllable and precisely maneuverable aircraft system.

The trim predictions and flight test results correlate well in Figure 8, with major differences being found only in the longitudinal cyclic angle. The reason is an interference effect between hub, fuselage and tailplane, which is not considered adequately in the analysis. Measurements of pressure distribution over the tailplane showed a severe dynamic pressure loss at the port side, which results from wake interference between main rotor hub, fuselage and tailplane. The static speed stability, i.e. longitudinal stick position vs. airspeed, proved to be very sensitive to small hub-fairing and tailplane modifications, as also indicated in Figure 8. More detailed information is given in Reference 1.

Control and stability characteristics were critically considered during the whole flight program. The stabilization of excessive flight conditions, as indicated previously, did not suffer under any control problems. Pilot comments point out that control power and control sensitivity remain excellent at these high airspeeds, without any discontinuity or adverse cross coupling effects. All controls have more than adequate displacement available in either direction. In particular, it was felt as beneficial, that by unloading the rotor due to wing lift the control power was not diminished. This gave the aircraft an excellent maneuver capability at all airspeeds.

Flight experience has further demonstrated, that the amount of instability of the hingeless rotor at high speeds can be tolerated by the pilots without any artificial stability augmentation. The handling characteristics are judged primarily from controllability and maneuverability. During the whole program there were never problems resulting from stability and control.

## 6. Aeroelastic Stability Characteristics

### 6.1 Aerodynamic Environment

Aeroelastic stability of a helicopter rotor blade in high speed flight is a multifarious problem due to the extreme variations of the aerodynamic environment of the advancing and retreating rotor blade. Compressibility effects at high Mach number and stall effects at high angle of attack can be identified as the

two causal elements that determine the rotor blade aeroelastic stability characteristics at high speeds.

An instructive picture of high speed aerodynamic environment is given in Figure 9, simulated flight condition corresponds to a 190 knots flight of the BO 105 HGH. For the position of the advancing blade there are shown the actual values of Mach number and flow angle of attack that are obtained at local elements of the blade. On the top of the diagram Schlieren photographs of those steady flow airfoil test points are shown, which were used for the calculation and which correspond to the  $M$ ,  $\alpha$ -conditions shown below. This diagram is intended to give a valid picture of the complex aerodynamic environment of the rotor at such extreme flight conditions. The state shown in Figure 9 is, of course, to be considered as a momentary picture of the azimuthally varying flow conditions. Critical combinations of incidence and transonic Mach-numbers are reached at early azimuth positions, giving a spanwise, chordwise, and azimuthal movement of shock fronts over wide parts of the advancing side. Nevertheless this picture should not leave the impression that the retreating blade aerodynamics are of less importance.

Because of the nonlinearity of all these processes coupled with the unsteady periodically varying aerodynamic environment at high advance ratio a proper estimation of the aeroelastic operational rotor limits is complicated. Hence, one of the principal objectives of the BO 105 HGH program was to explore the hingeless rotor aeroelastic stability characteristics at high speeds and to show the influence of blade airfoil modifications.

In the course of the HGH program the suspicion has been confirmed that under extreme forward flight conditions amplitude limited blade oscillations can be excited. These phenomena are of aeroelastic origin and able to couple with the airframe motions. They can have a restrictive effect on the operational flight envelope. Therefore, main emphasis is placed on the aeroelastic oscillations in high speed flight. A thorough discussion of the corresponding test data and first results of theoretical investigations are presented.

## 6.2 Standard Blade

During a high speed flight of 174 knots a subharmonic roll-vertical oscillation of the helicopter in connection with an amplitude limited tip-path-split of the rotor plane was observed. An oscillograph record of the airframe motions and of the control inputs is shown in Figure 10. The subharmonic content in the roll velocity trace is clearly identified.

Subsequent time and frequency analysis revealed that the inflight data of the rotor loads contain components with

rotor-harmonic-frequencies  $v\Omega$   
and rotor-subharmonic-frequencies  $(v + 0.5)\Omega$  ( $v = 0, 1, 2, \dots$ )

For example, Figure 11 shows typical plots of the vibratory pitch-link-load in the time and frequency domain. The flight conditions are characterized by the following nondimensional parameters:

$$\begin{aligned}\mu &= 0.415 \\ C_T/\sigma &= 0.097 \\ M_{1.90^\circ} &= 0.932.\end{aligned}$$

In addition to the multi-harmonic control loads there exist strong multi-subharmonic components. The simultaneous multi-subharmonic spikes in the amplitu-

de spectrum refer to a frequency modulation process which is typical for systems with periodic coefficients (see Reference 6).

The subharmonic blade excitation causes vibratory hub loads that transmit to the airframe. The predominant subharmonic roll-vertical-oscillations are explained by the proximity of the corresponding natural frequency.

A similar oscillation phenomenon was found during high speed flight tests of the Sikorsky NH-3A research compound helicopter (Reference 7) for advancing blade tip Mach numbers of above 0.92 and partially unloaded rotor.

Theoretical Studies: The analytical studies of the subharmonic tip-path-split phenomenon of the BO 105 HGH started with a sensitivity investigation of the aeroelastic blade behaviour for static pitching moment characteristics at high Mach numbers. In Reference 8, statically unstable characteristics were shown to be the principal sources of these phenomena.

The subharmonic blade oscillations were simulated using a rotor aeroelastic transient analysis with forward flight aerodynamics including stall, compressibility and three-dimensional effects (Reference 3). As a first result Figure 12 shows that the theoretical analysis is able to predict subharmonic blade oscillations for the BO 105 HGH, if

- the flight and trim conditions are carefully calculated and are in agreement to test conditions
- accurate and sufficient airfoil characteristics of the high subsonic Mach number region are available.

Evaluation of the results of the analytical simulation shows that rapid changes in pitching moments from statically stable to unstable conditions occur on the advancing blade tips at transonic Mach numbers. These shock-induced pitching moments influence the aeroelastic response at least via two different mechanisms:

- The moments generate a torsional forcing function that is independent of the blade motion.
- The moments affect the motion-dependent blade forces and can generate negative aerodynamic torsional stiffness.

The very nature of azimuthal and spanwise variation of the aerodynamic environment leads into a condition, where parametric-self-excitation primary in the blade torsional direction "superimposes" to the periodic forced blade excitation. The highly nonlinear pitching moment characteristics restrict the build-up of steadily growing blade oscillations and result in amplitude limited coupled aeroelastic blade oscillations in torsional, flapping, and lead-lag directions.

From the calculated time history of Figure 12 the subharmonic nature of the coupled blade-torsional oscillation as well as the mechanism of the tip-path-split phenomenon can clearly be seen. The large elastic torsional variation of  $\pm 2$  degrees at the advancing blade position ( $\psi = 90^\circ$ ) are inducing strong flapping responses, which have their maximum at the front of the rotor and are observed by the pilot as a separation of the tip-path plane. Results of a correlation study between theory and flight test are plotted in Figure 13. The agreement between the measured and calculated subharmonic blade flap-bending moments for two successive rotor revolutions is excellent.

### 6.3 Thin Tip Blades

During the high speed flight tests of up to 200 knots and advancing blade tip Mach numbers up to 0.96 the special subharmonic phenomenon, as encountered with the standard blades, could not be observed. However, a detailed post flight data analysis has uncovered again an unusual aeroelastic phenomenon, which occurred only under maneuver conditions. The phenomenon is characterized by the appearance of nonperiodic blade torsional/bending oscillations with distinct

rotor-harmonic frequencies  $v\Omega$   
and non-rotor-harmonic frequencies  $(v + 0.2)\Omega$ .  $v = 0, 1, 2, \dots$

Figure 14 shows plots of the time history and the corresponding amplitude spectrum of the vibratory pitch link loads measured at a slight pull-up maneuver at about 200 knots. The flight conditions are characterized by the non-dimensional parameters:

$$\begin{aligned}\mu &= 0.455 \\ C_T/\sigma &= 0.108 \\ M_{1.90^\circ} &= 0.925.\end{aligned}$$

In the load spectrum of Figure 14 there are now identified high non-rotor-harmonic spikes which partly exceed the normal harmonic content.

Studies were conducted to determine the physical conditions for the excitation of the non-rotor-harmonic oscillations of the AGB-I.

Additional Studies: To assess the effect of rotor thrust ( $C_T/\sigma$ ), a so-called short-time spectral analysis of the pitch link loads was made for the whole symmetrical pull-up maneuver. Figure 15 shows impressively the build-up of frequency-modulated control load spikes with load factor. During the maneuver the flight speed remained nearly constant. The growing control loads with increase of rotor  $C_T/\sigma$  is indicating the development of a stall-related limit cycle oscillation which is entirely different from that what is normally called rotor blade "stall flutter".

In order to clear up this statement more deeply, a typical control load time history and amplitude spectrum at high rotor thrust is plotted in Figure 16. The corresponding flight parameters are:

$$\begin{aligned}\mu &= 0.390 \\ C_T/\sigma &= 0.116 \\ M_{1.90^\circ} &= 0.880.\end{aligned}$$

The large spikes in the control loads appearing in the fourth quadrant of the blade azimuth are usually attributed to stall flutter, see Reference 9. As pointed out in References 9, 10 the high loads result from an aeroelastic self-excited pitching motion persisting only over small azimuth regions. Consequently the blade motions repeat periodically every revolution, manifested through the higher rotor-harmonic content in the spectrum of Figure 16. This type of stall-related phenomenon is identified in Reference 10 as excessive response.

After this discussion it becomes obvious that the observed limit-cycle oscillations of the thin tip blades in high speed flight cannot be explained exclusively by the generation of negative aerodynamic damping through successive dynamic stall-unstall cycles. But, if the aforementioned transonic pitching moment characteristics and their influence on blade torsional motion are taken into consideration, more light is shed on the problem. So the following line of reasoning for the occurrence of non-rotor-harmonic oscillations of the thin tip



blades can be developed by including the following three parameters simultaneously:

- Compressibility effects at the advancing blade with high tip Mach numbers ( $M_{1.900} > 0.92$ );
- Stall-related effects at the retreating blade under high rotor thrust conditions ( $C_T/\sigma > 0.09$ );
- Periodically varying aerodynamic environment ( $\mu > 0.44$ ).

The indicated three limit-conditions have been found necessary for the excitation of non-rotor-harmonic blade oscillations during the BO 105 HGH flight tests. This in fact explains the absence of these oscillation phenomena during the high speed flight tests with the winged helicopter version. For example Figure 17 shows the measured pitch link load spectra for steady dive conditions at 205 knots ( $\mu = 0.486$ ,  $M_T = 0.960$ ) and for the corresponding symmetrical pullout maneuver. The partially deloaded rotor has the expected beneficial effects of delaying the growth of non-rotor-harmonic spikes in the spectra.

#### 6.4 Interrelation of the Different Instability Phenomena

During the flight tests with both the standard and the thin tip blades the analysed instability phenomena were characterized by the excitation of distinct

non-rotor-harmonic-frequencies ( $v\Omega + \omega_{\text{mod}}$ ) for  $v = 0, 1, 2, \dots$ ,

where the modulation frequency  $\omega_{\text{mod}}$  was found to be

$$\omega_{\text{mod}} = \begin{cases} 0.5 & \text{for the standard blade} \\ 0.2 & \text{for the thin tip blade.} \end{cases}$$

The frequency difference cannot be attributed alone to the slightly different torsional natural frequencies of both blades, but should be related to the various aerodynamic profile characteristics. The present state of the art indicates that the aeroelastic instability phenomenon of the standard blade might be caused by a subharmonic resonance (see Reference 11) whereas that of the thin tip blade seems to be primary related to dynamic stall and is of a nonlinear flutter-type. In neither cases the excited blade oscillations become divergent, but they did cause extremely large torsional loads. Hopefully, further theoretical studies will give a more complete understanding of the observed aeroelastic blade oscillation phenomena.

#### 7. Conclusions

The following conclusions can be drawn from the results of the HGH high speed research program:

- With the BO 105 hingeless rotor system flight speeds of up to 200 knots for the pure helicopter and of 218 knots for the winged helicopter version in dive flight conditions have been demonstrated.
- Rotor bending and control loads are uncritical over the whole speed range, fatigue limits are only reached during excessive maneuvers. Theoretical load estimation is in good agreement with flight test data.
- Control sensitivity of the rotor system remains excellent in high speed flight and during maneuvers. Partial deloading of the rotor does not diminish control power. Inherent aircraft instability at high speeds can be tolerated without any type of artificial stabilization.

- An aeroelastic amplitude limited rotor oscillation experienced with standard blades in high speed flight (advancing-blade-tip Mach number of 0.93) had a restrictive effect on the operational flight envelope of the aircraft. With thin tip blades the aircraft was flown to higher speeds, with a similar type of oscillation occurring only under maneuver flight conditions. Furthermore, partial rotor deloading proved to be of highly relieving influence. A transient aeroelastic rotor analysis was successful in simulating this type of oscillations and in providing insight into parametric influences.
- The HGH high speed research program has demonstrated that the hingeless rotor is capable of operating in high speed flight regions of up to 220 knots. Certain aeroelastic phenomena which are mainly of aerodynamic origin, and hence not specifically inherent to hingeless rotors, can be solved by expanded theoretical investigations and by proper design work.

## 8. References

1. A. Teleki, High Speed Flight Tests with the BO 105 Helicopter. R. Ae. S. Rotorcraft Symposium, London (1975)
2. K.H. Hohenemser, Hingeless Rotorcraft Flight Dynamics. AGARD-AG-197 (1974)
3. G. Reichert, Loads Prediction Methods for Hingeless Rotor Helicopters. AGARD-CP-122 (1973)
4. G. Reichert and H. Huber, Influence of Elastic Coupling Effects on the Handling Qualities of a Hingeless Rotor Helicopter. 39th AGARD Flight Mechanics Panel Meeting on "Advanced Rotorcraft", Hampton Virginia (1971)
5. H. Huber, Effects of Torsion-Flap-Lag Coupling on Hingeless Rotor Stability. 29th Annual National Forum of the American Helicopter Society, Washington (1973)
6. M.A. Gockel, Practical Solution of Linear Equations with Periodic Coefficients. Journal of the AHS, Vol. 17, No. 1 (1972)
7. E.A. Fradenburgh, Flight Program of the NH-3A Research Helicopter. 24th Proceedings of the American Helicopter Society, Washington (1968)
8. W.F. Paul, A Self-Excited Rotor Blade Oscillation at High Subsonic Mach Numbers, Journal of the AHS, Vol. 14, No. 1 (1969)
9. R. Gabel and F. Tarzanin, Blade Torsional Tuning to Manage Large Amplitude Control Loads. J. Aircraft, Vol. 11, No. 8 (1974)
10. P. Crimi, Analysis of Helicopter Rotor Blade Stall Flutter. J. Aircraft, Vol. 11, No. 7 (1974)
11. G. Herrmann and W. Hauger, On the Interrelation of Divergence, Flutter and Auto-Parametric Resonance. Ingenieur-Archiv 42 (1973)



Figure 1 BO 105 - HGH with Hingeless Rotor in Flight



Figure 2 BO 105 - HGH (Winged Version) in Flight

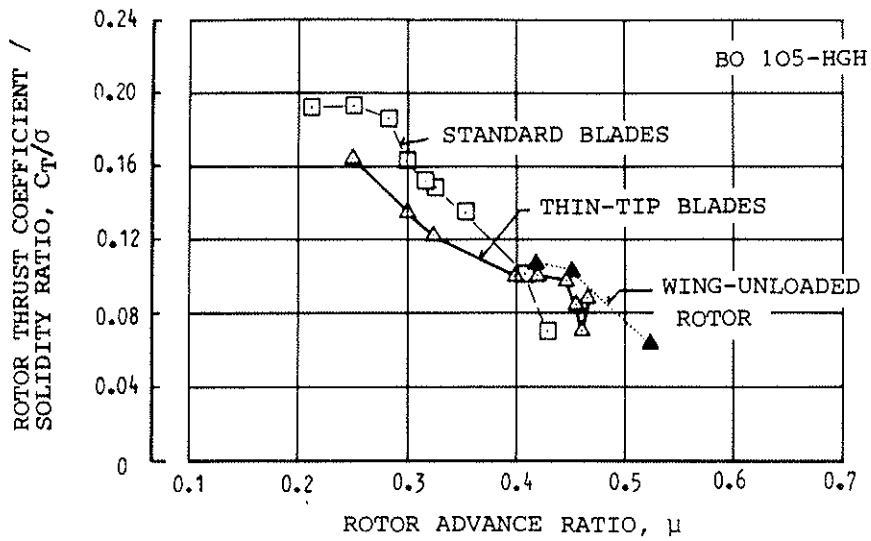


Figure 3 BO 105 - HGH Rotor Flight Test Envelope

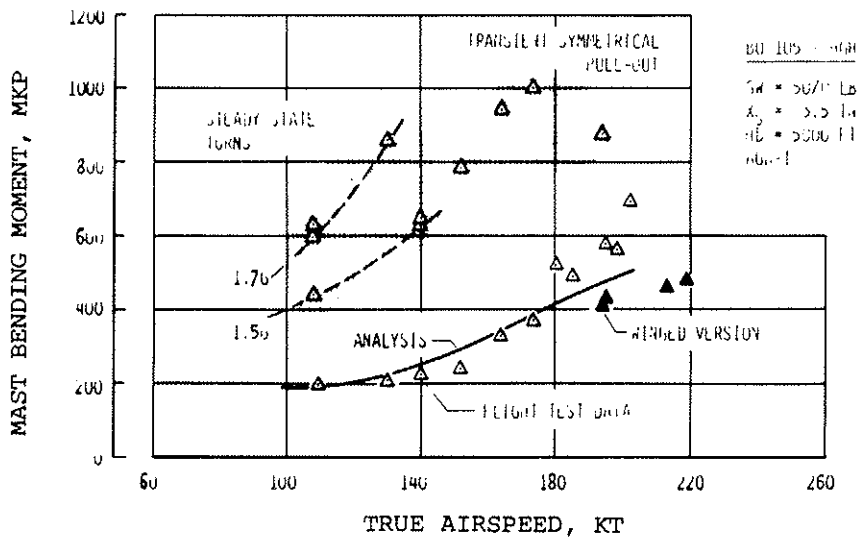


Figure 4 Mast Bending Moments in High Speed Flight and Maneuvers

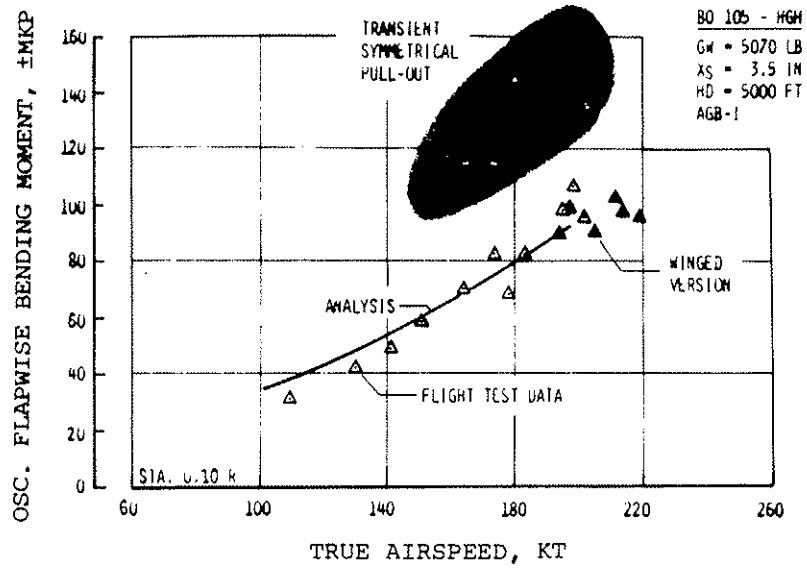


Figure 5 Oscillating Blade Root Flapwise Bending Moments over Airspeed and Maneuver Range

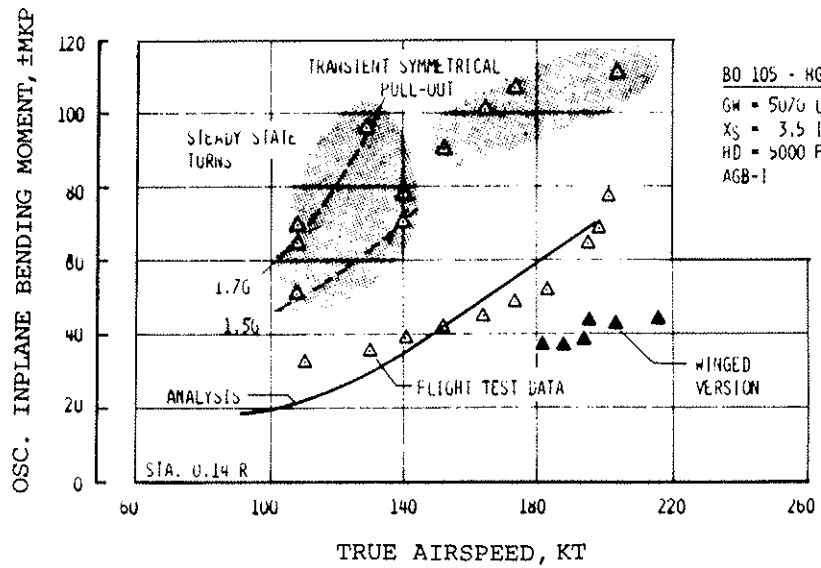


Figure 6 Oscillating Blade Root Inplane Bending Moments over Airspeed and Maneuver Range

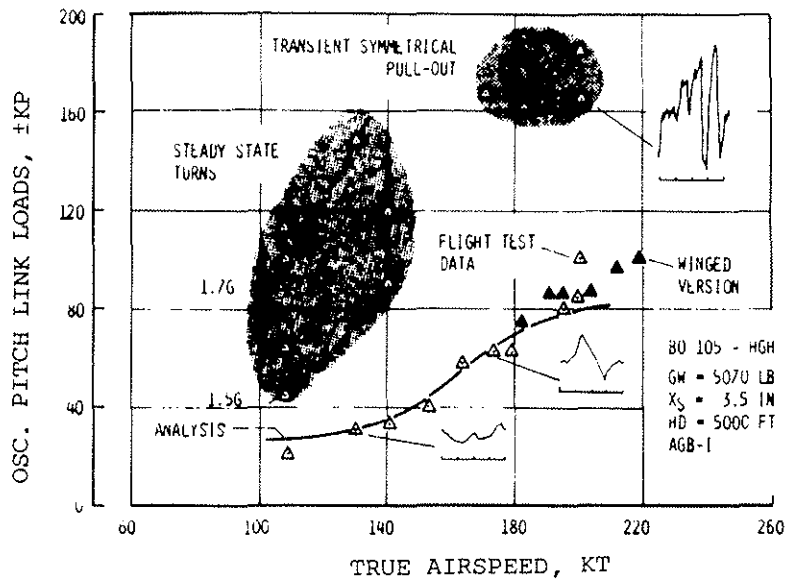


Figure 7 Oscillating Pitch Link Loads over Airspeed and Maneuver Range

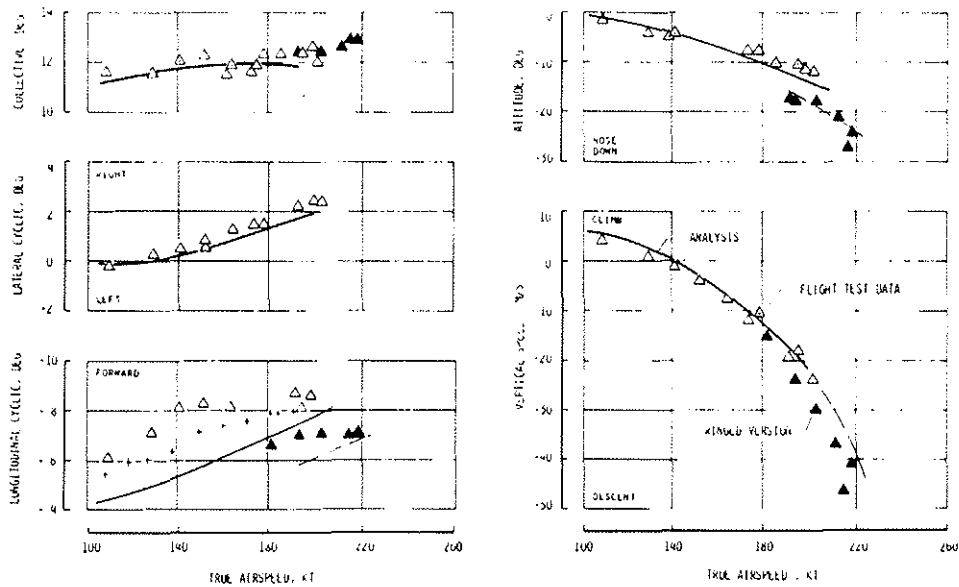


Figure 8 Trim Parameters in Flight with Constant Power Setting

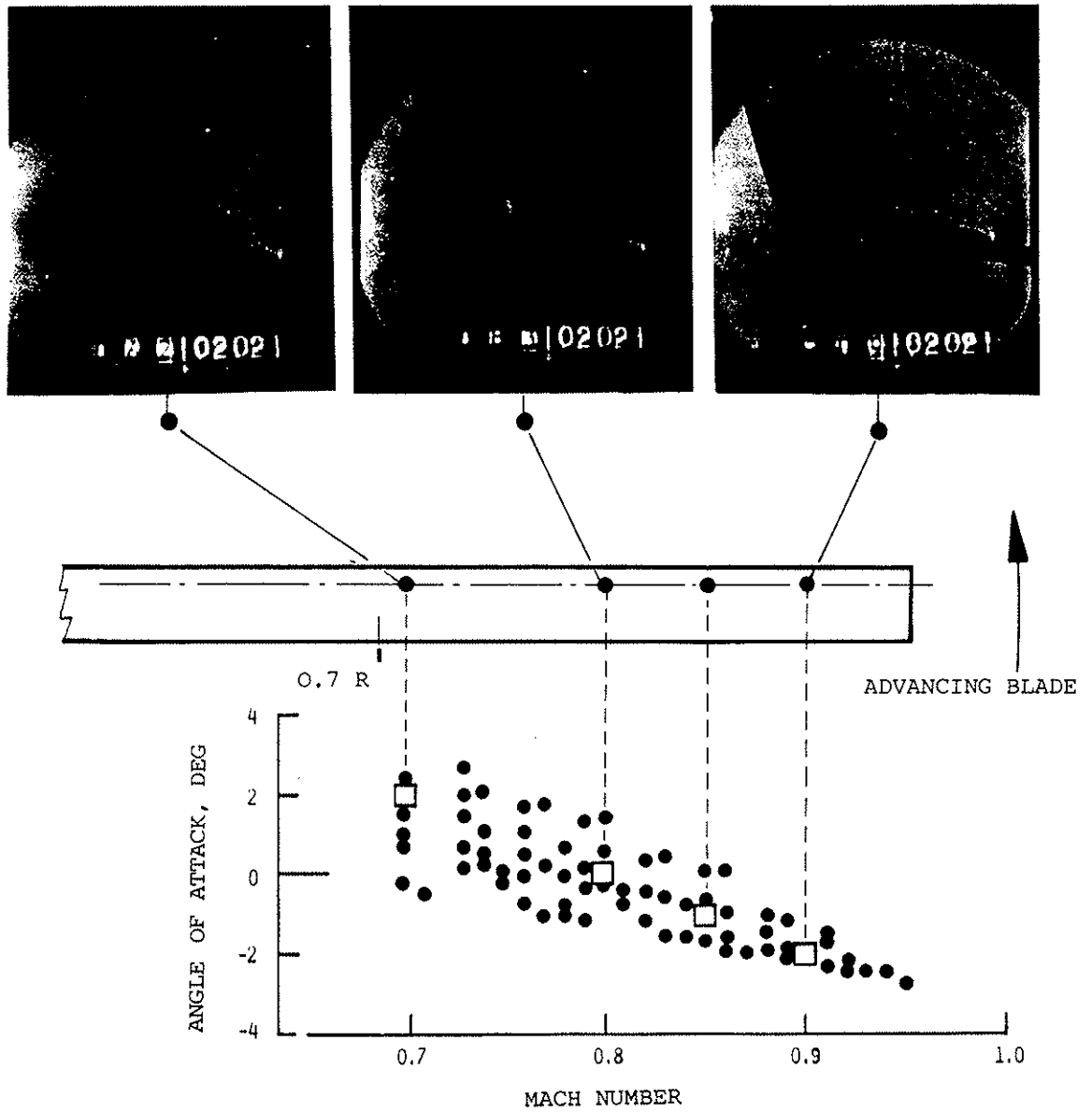


Figure 9 Simulated Aerodynamic Environment of the Advancing Blade (TAS = 190 knots)

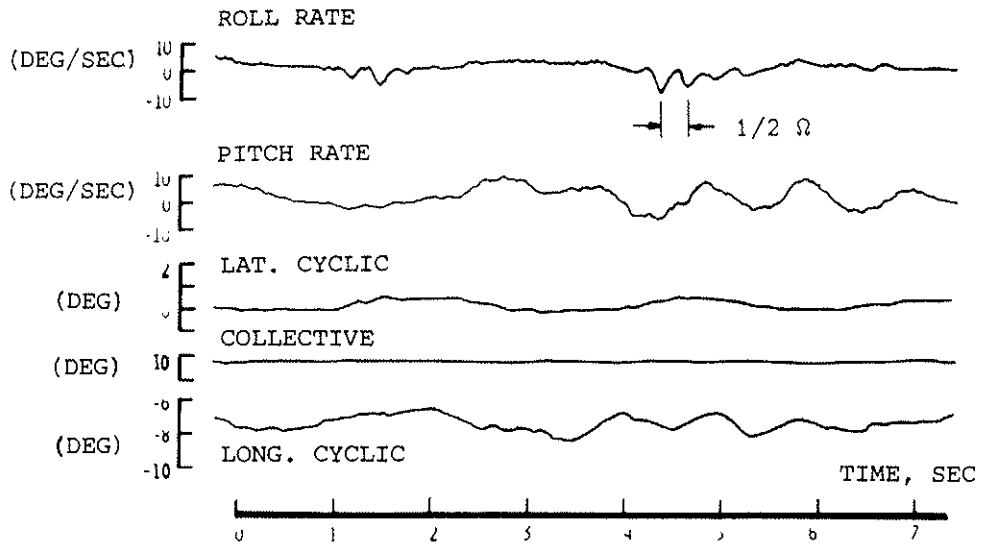


Figure 10 Subharmonic Aircraft Oscillation at 174 knots, BO 105 GHG with Standard Blades

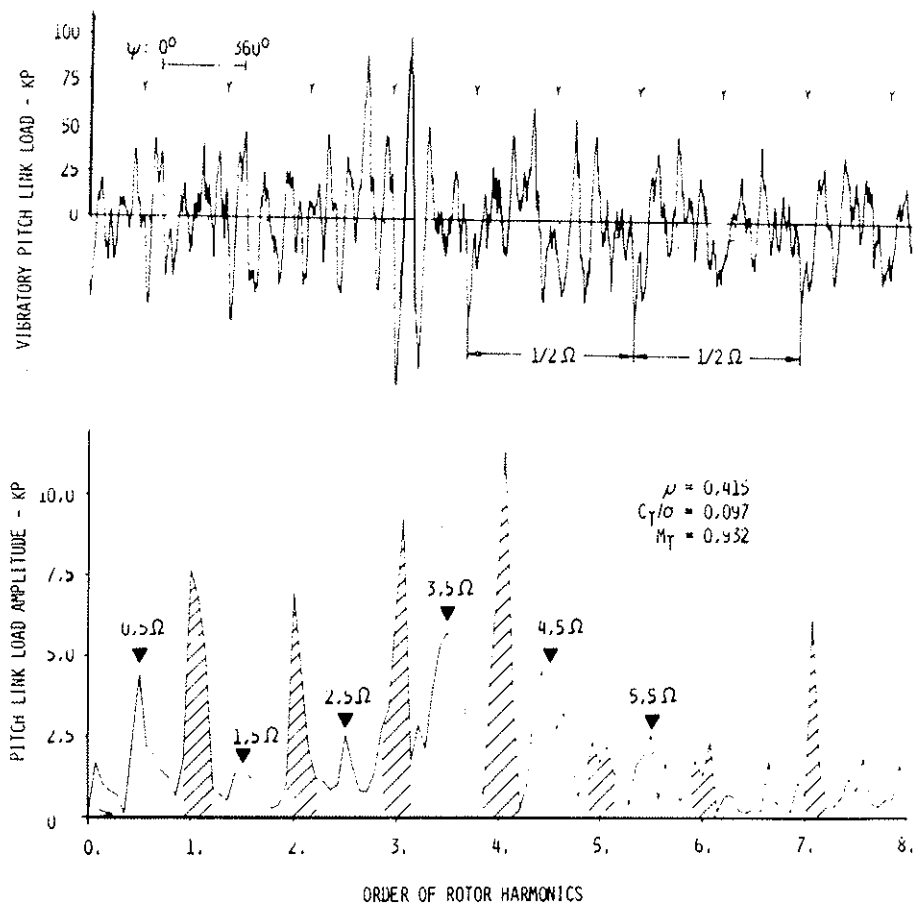


Figure 11 Waveform and Frequency Spectrum of Rotor-Subharmonic Control Loads with Standard Blades



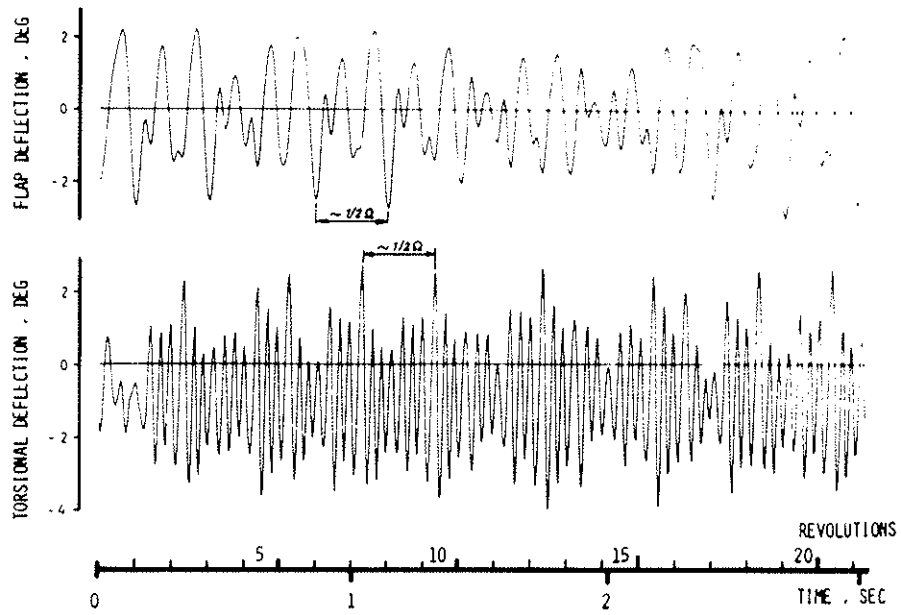


Figure 12 Subharmonic Flapwise and Torsional Blade Oscillation (Calculated)

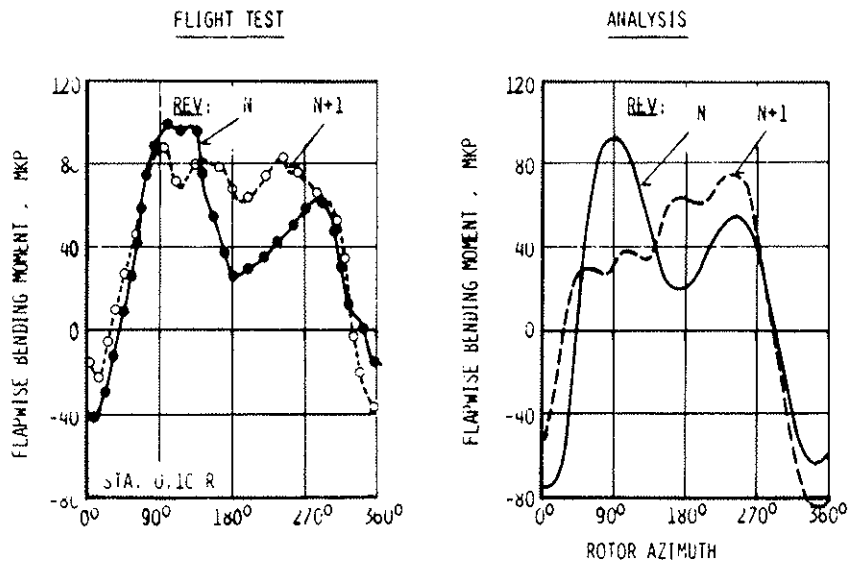


Figure 13 Subharmonic Flapping of a Rotor Blade, Comparison of Flight Test and Analysis

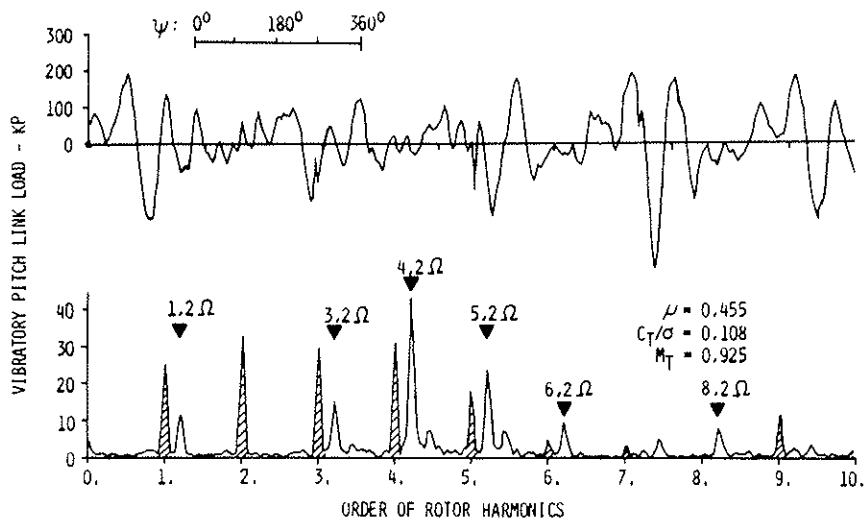


Figure 14 Waveform and Frequency Spectrum of Non-Rotor-Harmonic Control Loads with Thin Tip Blades

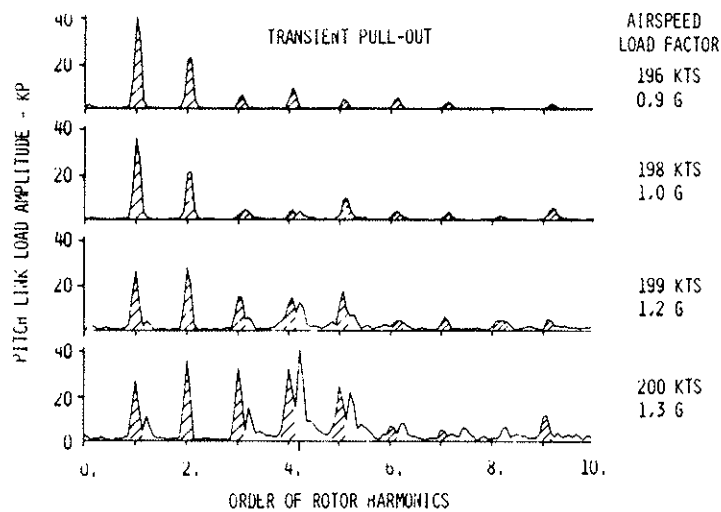


Figure 15 Growth of Non-Rotor-Harmonic Control Loads in Maneuvers (Thin Tip Blades)

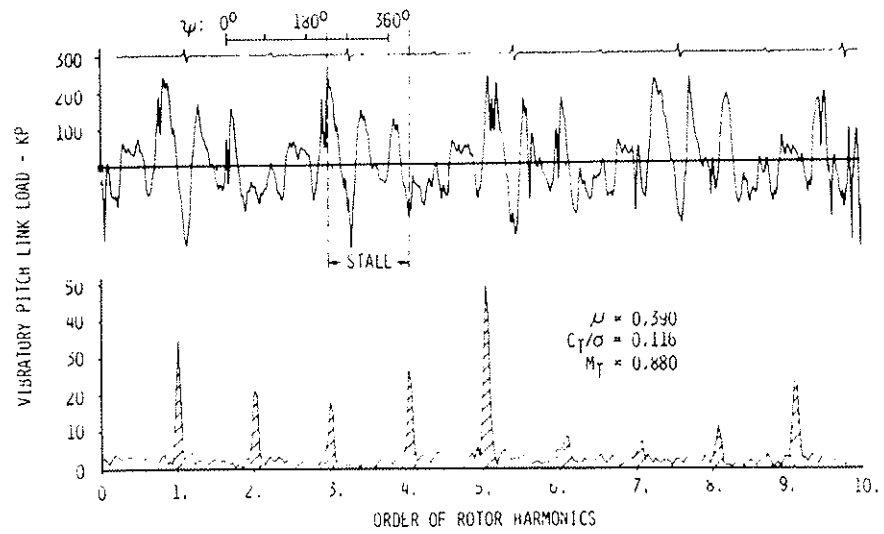


Figure 16 Waveform and Frequency Spectrum of Excessive Control Loads Due to Stall (Thin Tip Blades)

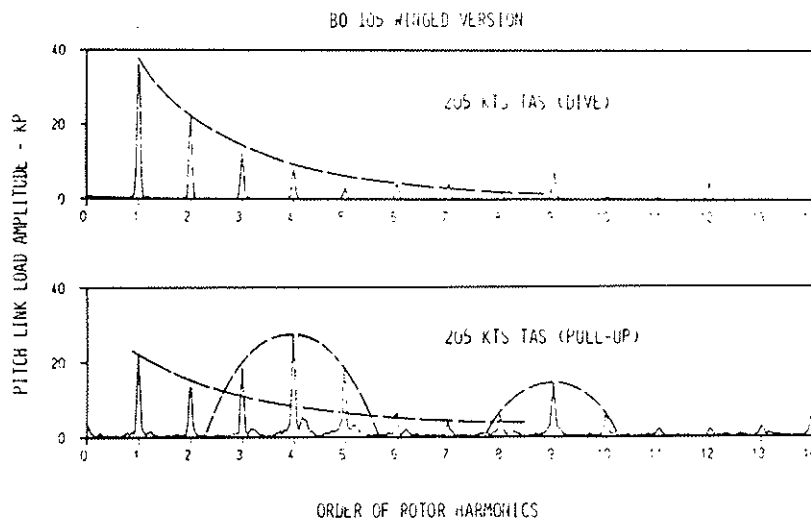


Figure 17 Control Loads Spectra in High Speed Flight (BO 105 - HGH Winged Version, Thin Tip Blades)